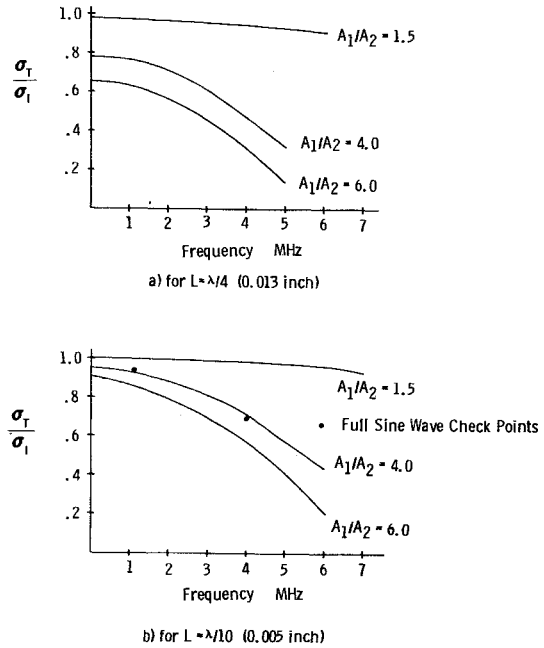

Fig. 2 Design curves—stress ratio vs frequency.

more of the input energy is transformed into the reflected modes of the propagating pulse through the discontinuity. Figure 2 presents the design curves developed from the results in Table 2. These design curves can be used as a tool to determine the loss in magnitude of the transmitted pulse for a given A_1/A_2 ratio and frequency value. These curves can also be used in the nondestructive testing of determining flaw sizes and voids as was suggested in Ref. 7.

The results of the third investigation verify that one computer run can be used to predict the effect of frequency on the stress ratio obtained in the second investigation with a big saving in computer runs. The results summarized in Table 3 show that good agreement is achieved between the two methods. The percent error varies from 3.64% to 5.28%, as indicated.

References

[1] Karl, F. C., "The Analogous Acoustical Impedance for Discontinuities and Constrictions of Circular Cross Section," *Journal of the Acoustical Society of America*, Vol. 25, No. 2, March 1953, pp. 327–334.

[2] Miles, J., "The Reflection of Sound due to a Change in Cross Section of a Circular Tube," *Journal of the Acoustical Society of America*, Vol. 16, No. 1, July 1944, pp. 14–19.

[3] Warburton, G. G. and Al-Mojafi, A. M. J., "Free Vibration of Thin Cylindrical Shells with a Discontinuity in the Thickness," *Journal of Sound and Vibrations*, Vol. 9, May 1969, pp. 373–382.

[4] Ripperger, E. A. and Abramson, H. N., "Reflection and Transmission of Elastic Pulses in a Bar of a Discontinuity in Cross Section," *Proceedings, Midwestern Conference on Solid Mechanics*, 3rd ed., 1957, pp. 135–145.

[5] Kenner, V. H. and Goldsmith, W., "One-Dimensional Wave Propagation Through a Short Discontinuity," *Journal of the Acoustical Society of America*, Vol. 45, No. 1, Aug. 1968, pp. 115–118.

[6] Mortimer, R. W., Rose, J. L., and Blum, A., "Longitudinal Impact of Cylindrical Shells with Discontinuous Cross-Sectional Area," *Journal of Applied Mechanics*, Vol. 39, No. 4, Dec. 1972, pp. 1005–1011.

[7] Rose, J. L. and Mortimer, R. W., "Elastic Wave Analysis in Nondestructive Testing," *Journal of Materials Evaluation*, Vol. XXXI, No. 3, March 1973, pp. 33–47.

[8] Mortimer, R. W. and Blum, A., "The Effect of Pulse Duration on the Transient Response of Cylindrical Shells Subjected to Axial Impact," *Journal of Applied Mechanics*, Vol. 41, March 1974, pp. 312–313.

MHD Augmented Shock Tunnel Experiments with Unseeded, High Density Air Flows

CLARENCE J. HARRIS* AND CHARLES H. MARSTON†
General Electric Company, Valley Forge, Pa.
AND
W. R. WARREN JR.‡
Aerospace Corporation, El Segundo, Calif.

Introduction

THE experimental study[1] referenced by Pate et al.[2] provides important and previously unpublished data which supports the feasibility of the high density, MHD augmented wind-tunnel concept. The results of this initial feasibility study are of particular interest in that they provide the only known available MHD augmented shock tunnel data obtained using unseeded air flows. Such operation more closely simulates real flight and eliminates the concern expressed[2] regarding flow seeding effects on model heat transfer, flow chemistry, and possible particle damage to models. This paper very briefly presents some additional measured MHD interaction effects flow data obtained from the earlier study in order to extend the scope of useful information available to interested investigators and wind tunnel users.

Discussion

This study was conducted using a high-performance electrically driven reflected shock tunnel. The unique performance capability of this type of shock driving technique permitted the generation of high pressure–high temperature shock tunnel reservoir conditions yielding highly ionized unseeded air flows in the accelerator and nozzle with moderate values of chemical dissociation.[3,4] The over-all facility setup is illustrated in Fig. 1. The design and performance of the MHD accelerator were based upon a one-dimensional, steady, inviscid, compressible flow analysis.[5] A typical set of calculated performance curves for this experiment is given in Fig. 2.

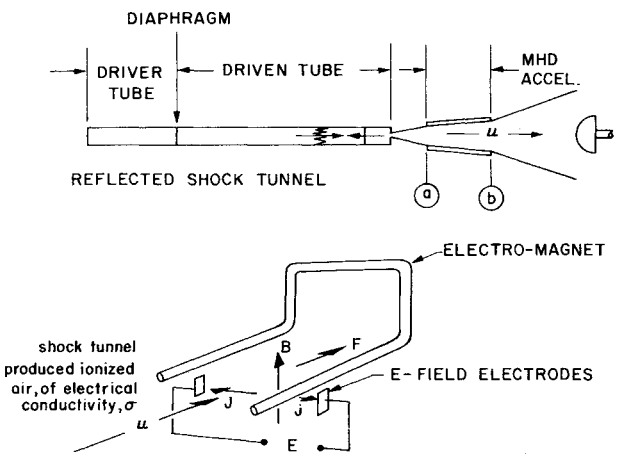

Fig. 1 Reflected shock tunnel-faraday MHD accelerator.

Received March 29, 1974; revision received August 20, 1974.
Index categories: Plasma Dynamics and MHD; Nozzle and Channel Flow.

* Physicist, Experimental Engineering (RESD).
† Senior Research Engineer, Space Sciences Lab. Member AIAA.
‡ Director, Aero and Propulsion Research Lab. Associate Member AIAA.

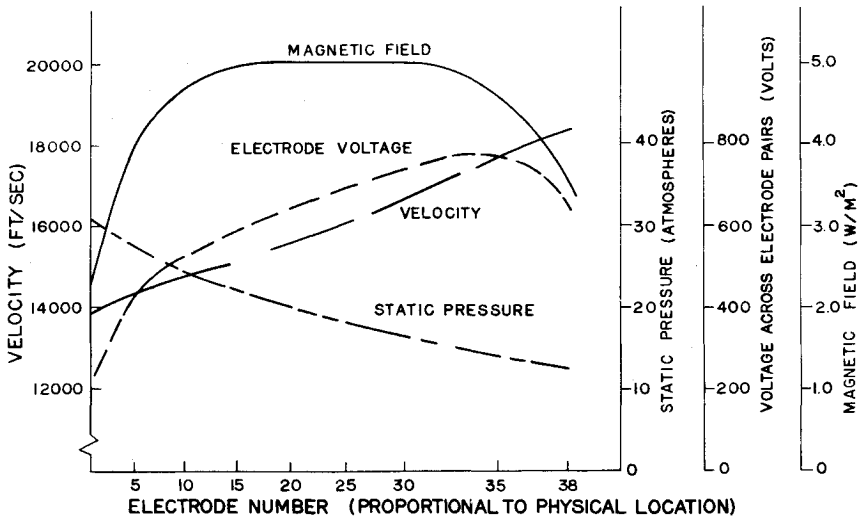

Fig. 2 Calculated properties through accelerator channel. High density inlet conditions, $K = E/UB = 1.85$, $\Delta h_o/RT_o = 103.4$, $\Delta S/R = 2.02$.

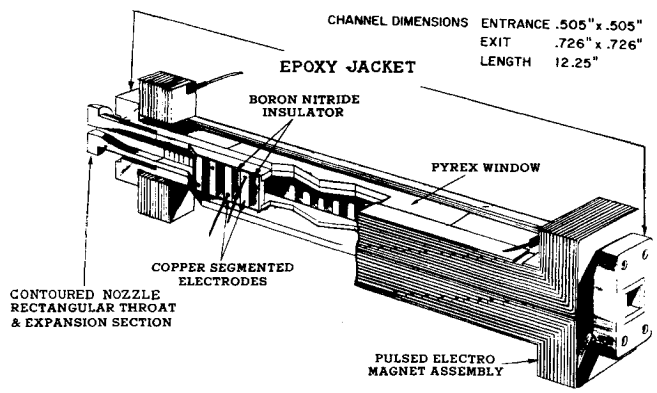

Fig. 3 Schematic drawing of channel and magnet assembly.

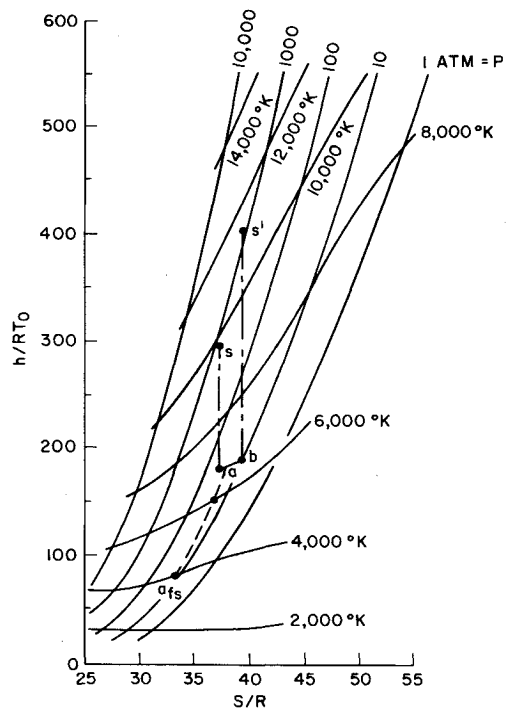

Fig. 4 Enthalpy/entropy increase due to MHD augmentation.

The MHD accelerator channel (Fig. 3) was 12.25 in. in length, had a square-cross-section (0.5 in. × 0.5 in. entrance), an area ratio of 2.0, with an average air electrical conductivity of 110 mho/m, at a nominal magnetic field strength of 5.2 W/m^2, resulting in an $LB^2\sigma/\rho v$, parameter value of 0.15. It has 38 pairs of segmented copper electrodes. It was experimentally determined[6] that the flow duration of ionized air in the accelerator was of the order of 300 μsec.§ The total MHD-augmented shock tunnel process is as illustrated in Fig. 4. The electrically arc-heated helium driver generates a strong shock wave ($M_s = 13.6$ at $P_1 = 150$ torr) which processes the air initially in the driven tube to the stagnation value S. This highly ionized air then expands isentropically to the MHD accelerator entrance a. The high-density ionized air is accelerated by the applied $J \times B$ forces; this kinetic energy addition being equivalent to raising the air stagnation enthalpy to S'. An increase in entropy also occurs during the MHD augmentation cycle. The air then further expands in the nozzle located downstream of the accelerator exit b, influenced by these increased entropy and effective stagnation enthalpy values.

The experimental performance was monitored by measuring accelerator wall voltage gradients normal to the flow, current-time history of various electrode pairs, channel static pressure, open circuit $U \times B$ induced potentials, and nozzle impact pressure. These measurements, with the exception of nozzle impact pressure, have been discussed in a limited manner in Refs. 7 and 8. From these measurements a direct determination of flow velocity increase due to MHD augmentation was obtained as well as an indication of over-all operational efficiency. A constant voltage electrode surface-sheath loss of approximately 100 V and a variable voltage cool boundary-layer loss that diminishes with increasing ohmic heating and/or turbulence of the boundary layer were postulated from these measurements.[9]

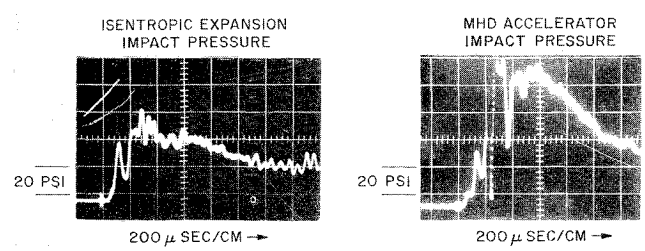

Fig. 5 Impact pressure measurements in the MHD accelerator.

§ Limited by the arrival of the driver expansion fan. The time to driver interface arrival is however 700 μsec.

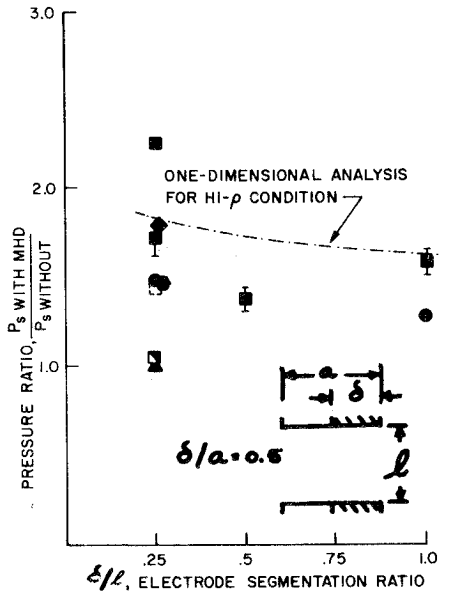

Fig. 6 MHD augmentation based on impact pressure increase, □-Hi-ρ; ○-MEDI-ρ; △-low enthalpy, unseeded, $B = 5.2$; ◇-low enthalpy, seeded, $B = 4.0$; ⬭-low enthalpy, seeded $B = 5.2$; filled symbols—fully powered MHD; dashed square—MHD Aug. @ 50% electric currents; half filled symbols—60% E-Field, no B-Field.

Operation of the facility under so-called "fully powered" conditions (as compared to "underpowered" conditions) eliminated the boundary-layer loss and resulted in an operational efficiency of 75% (somewhat below the 85%–90% value reported in Ref. 2).

Velocity increase data were obtained primarily from the impact pressure measurements. Fig. 5 shows nozzle impact pressure responses, and Fig. 6 is a summary of the wide range of impact data obtained compared to the one-dimensional analysis as a function of variation in MHD channel electrode segmentation ratio. The increase in impact pressure is quite pronounced and the analytically predicted increases in flow velocity were readily achieved experimentally. A tabulation of the various operational and flow conditions shown in Fig. 6 is given in Ref. 9 (Chart II). These conditions cover high and medium flow density (ρ), high and low reservoir enthalpy, and include a very limited study with seeded air using a novel "basket seeder."[9] Under the most optimum conditions used in this experiment, the velocity in the test section increased from 19,600 fps to 24,000 fps due to upstream MHD augmentation.

References

[1] Warren, W. R., et al., "Feasibility Study of High Density Shock Tunnel Augmentation by an MHD Accelerator," AEDC TR-62-225, Oct. 1965, Arnold Engineering Development Center, Tullahoma, Tenn.

[2] Pate, S. R., et al., "Development of an MHD-Augmented, High Enthalpy, Shock Tunnel Facility," *AIAA Journal*, Vol. 12, No. 3, March 1974, pp. 298–297.

[3] Warren, W. R. and Harris, C. J., "A Critique of High Performance Shock Tube Driving Techniques," *Proceedings of the 7th International Shock Tube Symposium*, Toronto, Ontario, Canada, 1969.

[4] Harris, C. J., "Comment on 'Nonequilibrium Effects on High-Enthalpy Expansion of Air'," *AIAA Journal*, Vol. 4, No. 6, June 1966, pp. 1148–49.

[5] Marston, C. H., "MHD Accelerator Performance for Specified Interaction Parameter," *AIAA Journal*, Vol. 4, No. 11, Nov. 1966, pp. 2078–2079.

[6] Harris, C. J., "Experimental Identification of Shock Tunnel Flow Regimes," *AIAA Journal*, Vol. 7, No. 2, Feb. 1969, pp. 365–369.

[7] Harris, C. J., et al., "Measuring Techniques Applied in Determining the Performance of an MHD Augmented Shock Tunnel," *IEEE Transactions on Aerospace and Electronic Systems*, Vol. AES-3, No. 3, May 1967, pp. 433–440.

[8] Harris, C. J., et al., "MHD Generator and Accelerator Experiments in Seeded and Unseeded Air Flows," *Transactions on International Electricity from MHD Symposium*, Vol. 1, International Atomic Energy Agency, Salzburg, 1966.

[9] Harris, C. J., "MHD Augmented Shock Tunnel Study," AEDC TR-68-161, Aug. 1968, Arnold Engineering Development Center, Tullahoma, Tenn.

Interpolation in Numerical Optimization

KENNETH R. HALL* AND DAVID G. HULL†
The University of Texas at Austin, Austin, Texas

A NUMBER of numerical optimization methods, for example, the gradient method, the generalized perturbation method,[1] and quasilinearization, iterate on variable histories. In order to facilitate the updating process from one iteration to the next, a fixed-step, multistep integrator, such as the Adams-Moulton, Adams-Bashforth integrator, is normally used. With a low-order integrator, say fourth order, it may be necessary to use a large number of integration steps to get the accuracy needed to achieve convergence, and this is costly with respect to both computer time and computer storage. At the same time, a large number of integration steps can lead to round-off error in the numerical integration process. The problems previously mentioned can be circumvented by using a variable-step integrator with stepsize control based on local relative truncation error. However, this procedure requires the use of an interpolation method because the pattern of integration steps will differ from one iteration to the next. In addition, the orders of the interpolator and the integrator must be similar to achieve the desired accuracy. One arrangement which has been used successfully[1,2] is the Runge-Kutta-Fehlberg 3(4) integrator[3] and the cubic-spline interpolator. The purpose of this Note is to discuss the cubic-spline interpolator in terms of the requirements imposed by numerical optimization.

In general, the requirements imposed on the cubic-spline interpolator by numerical optimization are that the spline be generated accurately and with the minimum amount of storage. The standard procedure for generating a spline involves the solution of a linear system in which the coefficient matrix is tridiagonal. The linear system can be solved by an elimination method (for example, Gauss elimination) or by an iterative method (for example, successive over-relaxation). With regard to accuracy, both methods yield essentially the same results. However, Gauss elimination requires the storage of three more N-vectors than successive over-relaxation, where N is the number of nodal points. If N is large and if several curves are being interpolated, storage minimization makes iterative methods more attractive than elimination methods. It should be mentioned, however, that iterative methods usually require more computer time.

An algorithm and a code for generating the cubic spline with successive over-relaxation is presented in Ref. 4. However, there are two aspects of the procedure used in Ref. 4 which

Received April 17, 1974; revision received September 10, 1974. This research was supported by NASA/MSC Contract NAS 9-11964.

Index category: Navigation, Control, and Guidance Theory.

* Assistant Professor of Aerospace Engineering and Engineering Mechanics.

† Associate Professor of Aerospace Engineering and Engineering Mechanics. Member AIAA.